Poster #: 1016

XXI IWCLL International Workshop on CLL

Integrating phospho-proteomic analysis and innovative 3D cell culture systems to dissect the role of extracellular stiffness in CLL pathogenesis

Marco Cellani[1], Riccardo Pinos[1], Margherita Pauri[1] , Matteo Pitton[1], Federica Barbaglio[1], Anna Sofia Tascini[4], Lydia Scarfò[2,5], Silvia Farè[3], Paolo Ghia[2,5] and Cristina Scielzo[1]

[1] Division of Experimental Oncology, Malignant B cells biology and 3D modelling Unit, San Raffaele Hospital (IRCCS), Milan, Italy.

[2] Division of Experimental Oncology, B cell neoplasia Unit and Strategic Research Program on CLL, San Raffaele Hospital (IRCCS), Milan, Italy.

[3] Department of Chemistry, Materials and Chemical Engineering, Politecnico di Milano, Milan, Italy.

[4] Center for Omics Sciences, San Raffaele Hospital (IRCCS), Milan, Italy.

[5] School of Medicine, Università Vita-Salute San Raffaele, Milan, Italy.

OBJECTIVE

- Investigate the impact of mechanical cues, particularly focusing on extracellular stiffness variation, on the pathogenesis of CLL cells.

CONCLUSIONS

- CLL cells experience **tissutal stiffness in 3D settings**, potentially impacting their viability and transcriptomic profile.
- 3D bioprinted CLL primary cells showed an **increased resistance** to therapies compared to 2D condition.
- We identified a **range of stiffness** that affects CLL cells activation.
- Characterization of MEC1 cells under mechanical stimulation revealed modulation of intracellular pathways potentially involved in novel pathogenic mechanisms (**Ephrin signaling pathway**), along with concurrent regulation of the upstream signal (**VLA-4 antigen**). The same experiments are **ongoing in primary CLL cells**.

REFERENCES

1. Sbrana FV, Pinos R, Barbaglio F, et al. 3D Bioprinting Allows the Establishment of Long-Term 3D Culture Model for Chronic Lymphocytic Leukemia Cells. Front Immunol. 2021;12:639572. Published 2021 May 3. doi:10.3389/fimmu.2021.639572
2. Ribezzi D, Pinos R, Bonetti L, Cellani M, Barbaglio F, Scielzo C and Farè S (2023), Design of a novel bioink suitable for the 3D printing of lymphoid cells. Front. Front. Biomater. Sci. 2:1081065. doi: 10.3389/fbiom.2023.1081065
3. Sampietro M, Cellani M, Scielzo C. B cell mechanobiology in health and disease: emerging techniques and insights into therapeutic responses. FEBS Lett. Published online May 19, 2025. doi:10.1002/1873-3468.70071
4. Zhang X, Cao D, Xu L, et al. Harnessing matrix stiffness to engineer a bone marrow niche for hematopoietic stem cell rejuvenation. Cell Stem Cell. 2023;30(4):378-395.e8 doi:10.1016/j.stem.2023.03.005
5. Qin Q, Wang D, Xu L, Lan Y, Tong M. Evaluating Lymph Node Stiffness to Differentiate Bacterial Cervical Lymphadenitis and Lymph Node-First Presentation of Kawasaki Disease by Shear Wave Elastography. J Ultrasound Med. 2021;40(7):1371-1380. doi:10.1002/jum.15518
6. Pasquale EB. Eph receptors and ephrins in cancer: bidirectional signalling and beyond. Nat Rev Cancer. 2010;10(3):165-180. doi:10.1038/nrc2806
7. Alonso-C LM, Trinidad EM, de Garcillan B, et al. Expression profile of Eph receptors and ephrin ligands in healthy human B lymphocytes and chronic lymphocytic leukemia B-cells. Leuk Res. 2009;33(3):395-406. doi:10.1016/j.leukres.2008.08.010

ACKNOWLEDGMENTS

This project recieved the financial support from AIRC - Fondazione AIRC per la Ricerca sul Cancro under: IG 2023 – ID. 28750. Figures have been created with BioRender.com

DISCLOSURES

Nothing to disclose

BACKGROUND

1. 3D bioprinting improves viability, transcription profile and affects drug response of CLL cells

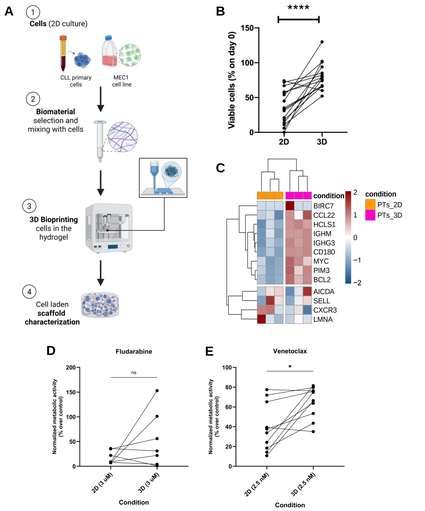

➢ **A)** Schematic representation of the 3D bioprinting workflow. **B)** Cell viability of 2D cultured and 3D bioprinted CLL primary cells on day 7 (n=16); Paired t test (*p<0.05) (**Ref. 1**). **C)** Heat-map of the most variable genes among 2D cultured and 3D bioprinted CLL primary cells (**Unpublished**). **D)** Percentage of metabolically active CLL primary cells in 2D and 3D following drug treatment with Fludarabine for 72 hours (n=7); Paired t test (*p<0.05) (**Unpublished**). **E)** Percentage of metabolically active CLL primary cells in 2D and 3D following drug treatment with Venetoclax for 24 hours (n=10); Paired t test (*p<0.05) (**Unpublished**).

2. Scaffold with CLL cells mimic lymphoid organ stiffness

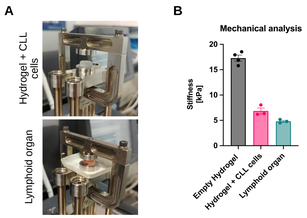

➢ **A)** Representative images of mechanical analysis conducted on scaffolds and a lymphoid organ (**Ref. 2**). **B)** Average and standard deviation values of stiffness for the scaffolds and the lymphoid organ (n=3).

3. Implication of physical cues on B cells in health and disease

READ THE PAPER

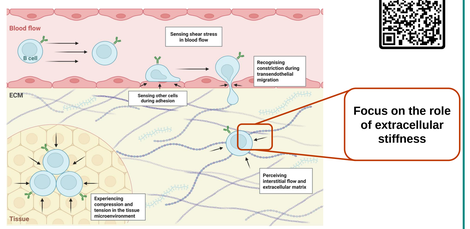

➢ Circulating B lymphocytes are subjected to a wide range of physical cues, which they can convert to biochemical signals through mechanotransduction (**Ref. 3**).

METHODOLOGICAL APPROACHES & RESULTS

➢ CLL cell line **MEC1** have been cultured on **stiffness-controlled plates**. Following 1 hour adhesion, **attached** cells have been recovered and deeply characterized.

1. Experimental workflow

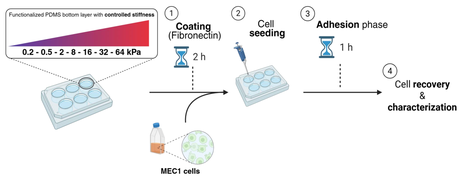

➢ CLL cell line were cultured in a controlled 2D system with defined rigidities (*Advanced BioMatrix*). Attached cells have been recovered after 1 hour of culture for characterization.

2. MEC1 cells characterization upon mechanical stimulation

A. Cell viability is maintained among all the conditions

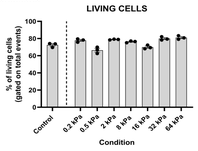

B. IgM is upregulated between 0.5 and 8 kPa

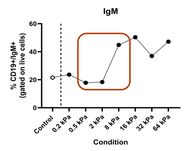

C. CD23 is downregulated at 8 kPa

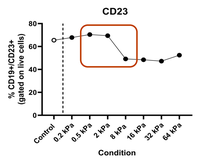

D

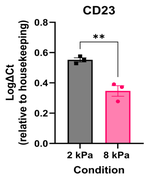

E. CD62L downregulation has been observed in the same range (0.5 – 8 kPa)

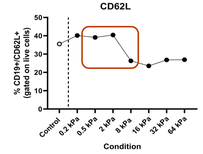

F

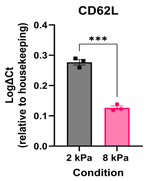

➢ **A)** Percentage of viable CLL cells attached to stiffness-tunable substrates. **B)** Percentage of IgM/CD19 +/+ CLL cells collected from the surface. **C)** Percentage of CD23+/CD19+ CLL cells collected from the surface. **D)** CD23 expression of CLL cells, measured by RT-qPCR; Paired t test (*p<0.05). **E)** Percentage of CD62L+/CD19+ CLL cells collected from the surface. **F)** CD62L expression of CLL cells, measured by RT-qPCR; Paired t test (*p<0.05).

3. Stiffness range identification for 3D bioprinting and following readouts

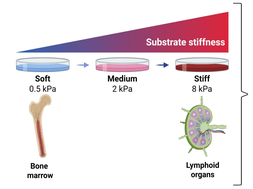

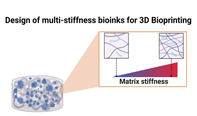

➢ Stiffness range identified after characterization (**Ref. 4-5**). The range will be exploited for the development of hydrogel with tunable biomaterial stiffness, suitable for 3D bioprinting (**Manuscript in preparation**).

READOUT	CONDITION
- Antigen expression profile (**Flow cytometry**) - Kinase activity (**Phospho-proteomic analysis**) - Protein expression (**Western Blot**)	- **CONTROL A**: cells in suspension - **CONTROL B**: cells adhering to plastic (K = 2 gPa) - **STIFFNESS**: 0.5 kPa - 2 kPa – 8 kPa

4. VLA-4 antigen is modulated by MEC1 cells upon culture on different rigidities

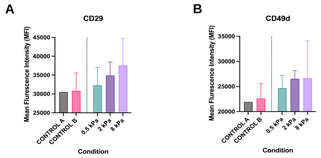

➢ **A)** CD29 marker expression, measured by Mean Fluorescence Intensity (MFI) (n=3). **B)** CD49d marker expression, measured by Mean Fluorescence Intensity (MFI) (n=3).

5. Phospho-proteomic revealed modulation of pathways potentially involved in disease pathogenesis

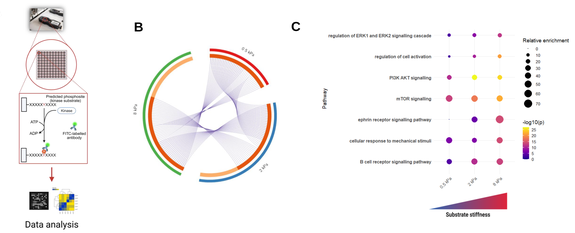

➢ **A)** Schematic representation of the protein tyrosine kinase activity assay (*Pamgene International B.V.*). **B)** Protein overlap analysis showing the significantly modulated kinases shared among the condition. **C)** Enrichment analysis of selected pathway obtained from kinase analysis.

➢ **Ephrin** receptor signaling pathway (GO: 0048013) was found to be significantly enriched at higher rigidities (2 and 8 kPa) and not significantly modulated during adhesion to softer substrates (0.5 kPa) (**Ref. 6-7**).

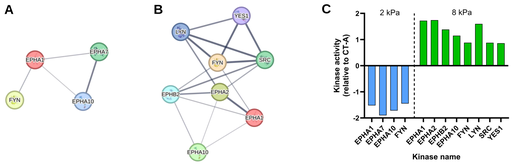

➢ **A)** Network analysis showing kinase belonging to Ephrin receptor signaling pathway modulated at 2 kPa condition compared to CONTROL A. **B)** Network analysis showing kinase belonging to Ephrin receptor signaling pathway modulated at 8 kPa condition compared to CONTROL A. **C)** Kinase activity (relative to CONTROL A) of proteins belonging to Ephrin signaling pathway, significantly modulated at 2 kPa and 8 kPa condition.

6. Kinase activation assessment confirms the changes observed by phospho-proteomic analysis

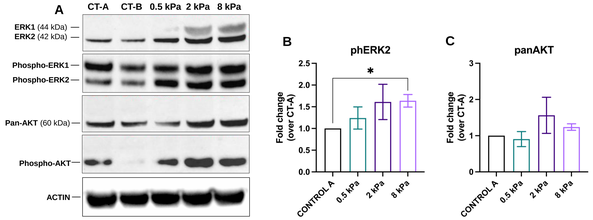

➢ **A)** Representative Western Blot of ERK1/2, phERK1/2, panAKT and phAKT proteins expressed by MEC1 cells upon culture stiffness-controlled substrates. **B)** Fold change expression of phospho-ERK2 (normalized on ACTIN) compared to CONTROL A condition (n=3); One-sample t and Wilcoxon test (*p<0.05). **C)** Fold change expression of panAKT (normalized on ACTIN) compared to CONTROL A condition (n=3); One-sample t and Wilcoxon test (*p<0.05).